Load-bearing capacity of circular, pointed and elliptical masonry arches

Danila Aita[1], Riccardo Barsotti[2], Stefano Bennati[2]

[1]*Dipartimento di Scienze per l'Architettura, Università di Genova, Italy*
[2]*Department of Civil Engineering, University of Pisa, Italy*
e-mail: *r.barsotti@ing.unipi.it, s.bennati@ing.unipi.it*

Keywords: Masonry arches, Nonlinear elastic analysis, Limit analysis.

SUMMARY. The paper illustrates some results on a comparative evaluation of the load bearing capacity of three different types of masonry arches subjected to their own weight and the weight of an overlying vertical wall masonry. The arch types considered are those most commonly found in historical masonry buildings and bridges: circular, pointed and elliptical. The analyses have been conducted using two different complementary methods: the first a simple extension of the Durand-Claye stability area method; the second based on application of a non-linear elastic one-dimensional model, already used by the authors in prior studies. In all cases, it is assumed that the arch's constituent materials has limited compressive strength and is unable to transmit tensions. In addition, the load transferred to the arch by the overlying wall is determined under the assumption that each vertical strip of wall bears directly down on the underlying arch element. Preliminary results reveal the clearly greater bearing capacity of the pointed arch with respect to the other types, thereby confirming a widely held conviction.

1 INTRODUCTION

Circular (round), pointed (ogival) and elliptical arches are found in many masonry buildings and bridges. It therefore appears interesting to examine the composite systems made up of the arch and overlying wall in buildings, and by the arch and filling material, paving and spandrel walls, in bridges. The aim is to determine the stress levels as a function of the main geometrical and mechanical parameters, and thereby assess the safety margin under conditions of incipient collapse, as well as the actual mechanism by which such collapse would occur.

Determining the structural response of such structures, in terms of both displacements and stresses, still represents a challenging task because of the strong non-linearity of masonry's behavior. Consequently large-dimension, numerical analysis are commonly utilized in achieving a solution [1], [2]. Here a simplified version of the problem will be addressed by following the two different approaches described and focusing on the arch alone. The first is based on an expressly developed extension of Durand-Claye's stability area method [3] and aims at determining the set of statically admissible solutions within the limits imposed by the ultimate compressive and tensile strengths and the limited shear capacity of the joints. When such set becomes empty, a limit equilibrium condition is attained for the whole system. The second approach instead studies the stress and strain fields generated in the arch, which is considered to be made of material offering poor resistance to tension. Such mechanical behavior can be modeled, as a first approximation, via a non-linear elastic constitutive relation, in which case the problem is tackled by studying and numerically integrating systems of non-linear equations [4]. The condition of incipient collapse is considered to be reached when the residual stiffness of the system falls below a predetermined

fraction of its initial value.

The results are presented in terms of a comparison between the load-bearing capacities of circular, pointed and elliptical arches, as estimated by both methods. As already observed in previous cases studied by the authors [5], the results obtained via these two methods of analysis turn out to be in excellent agreement, except for very few special cases. Moreover, the two methods perform complementary functions: the stability area method allows for readily determining a collapse load value, while the non-linear elastic analysis provides a helpful and, in some aspects, essential check of its mechanical significance by following the evolution of the displacement field and extension of the non-linear regions where cracking and crushing phenomena arise as the load increases.

2 THE ARCH-WALL SYSTEM

In this paper we consider the equilibrium problem of circular, elliptical and pointed masonry arches subject to their own weight and to the weight of a superimposed wall (Figure 1).

With the aim of making a first comparison between the load-bearing capacities of arches characterized by different shapes, in all the cases we have assumed a clear arch span L = 10 m. In addition to the circular arch, two elliptical arches of architectonic interest have also been considered: the first is defined by $a = L/2$ = 5 m, and b = 3.78 m, where $2a$ and $2b$ indicate the lengths of the axes of the intrados ellipse (Figure 1); the second arch is a depressed arch with semi-axes $a = L/2$ = 5 m, b = 1 m. Regarding the pointed arch, a rise-to-span ratio of $\sqrt{3}/2$ has been chosen. In all cases we have assumed a compressive strength σ_c = 20 MPa, a tensile strength $\sigma_t = 0$ and a Young's modulus E = 4 GPa.

With the aim of investigating the effects on the solution produced by variations in the shapes of both the arch and the wall, we have considered different values for the arch's thickness h and the angle β formed between the extrados of the wall and the horizontal direction. All the different types of arches are assumed to have horizontal springings and constant thickness.

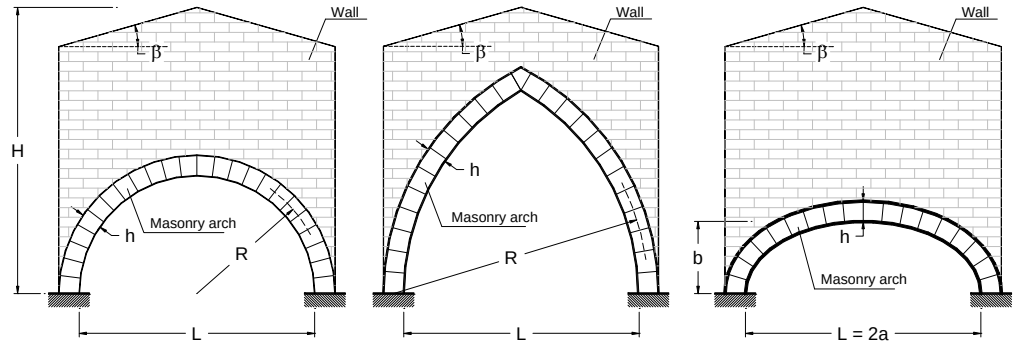

Figure 1. Scheme of the arch-wall systems
for circular (left), pointed (center) and elliptical (right) arches.

For different values of β and arch thickness h we have determined the maximum height of the wall compatible with the load-bearing capacity of the arch, the corresponding stress and strain distributions, the cracking pattern within the arch and the displacement field, by studying both the progressive reduction of the stability area and the evolution of the non-linear elastic solution. In all

cases *the superimposed wall is treated as a dead vertical load acting on the masonry arch*: in other words, we assume the wall to be divisible into vertical strips, the weight of each being directly sustained by the underlying arch element. This simplifying assumption, commonly adopted in the literature, has been dealt with in detail and examined critically in [6].

Lastly, it is worth noting that the 'limit condition' takes on a different meaning depending on whether we adopt the 'stability area' method or the non-linear elastic analysis: according to the first, it corresponds to the attainment of a 'limit equilibrium' state, while in the second, it is related to the vanishing of the arch residual stiffness.

3 THE SOLUTION METHODS

3.1 *The stability area method*

The stability area method is a derivation of Durand-Claye's method: a graphical procedure to determine the so-called area of stability at the crown section of a symmetrical arch, that is to say, the area within which the extremes of the vectors representing the crown thrust must be included in order that both the global equilibrium of the structure and the limited strength of masonry be respected. Here we provide only a brief qualitative description of the method; further details can be found in some previous works (see, for example, [7]), which present an extension of Durand-Claye's original method in order to account for any tensile and compressive strength of the masonry.

Let us now consider a symmetrical masonry arch, with finite compressive strength σ_c and zero tensile strength, and examine the ideal voussoir comprised between the crown joint c_0d_0 and a generic joint c_id_i (Figure 2). Let $W(\theta_i)$ be the weight of the voussoir $c_0d_0d_ic_i$, $N(\theta_i)$ the axial force at the joint c_id_i, P the thrust at the crown section and e the eccentricity of its application point.

Assuming the usual linear law for the compressive stress distribution, we can draw the area $c_i\omega_id_i$, each point of which corresponds to an admissible value of the axial force $N(\theta_i)$ with respect to the strength σ_c, and the corresponding hyperbola α_i and β_i at the crown joint, obtained by imposing the equilibrium of the voussoir $c_0d_0d_ic_i$.

The admissible thrusts P with respect to equilibrium and strength at the joint c_id_i are then represented by the horizontal vectors whose extremes are contained within the area $r_is_ip_iq_i$, delimited by the hyperbola α_i and β_i, and the curves $c_0\omega_0$ and $d_0\omega_0$.

To account for the friction at joint c_jd_j it is sufficient to draw at a generic point a the friction cone, defined by the friction angle φ (Figure 2). Let us take the weight $W(\theta_j)$ applied at point a and consider the two horizontal thrusts which give a resultant coinciding with the boundaries of the cone. These thrusts define two vertical lines at the crown, which encompass the extremes of the vectors representing the admissible thrusts P for the translational equilibrium along c_jd_j.

Then, to assure both equilibrium and respect of the limit conditions for the compressive stresses and friction along the joint c_id_i, the admissible thrusts at the crown will be comprised within the intersection A_i of the area $r_is_ip_iq_i$ with the two vertical lines defined above.

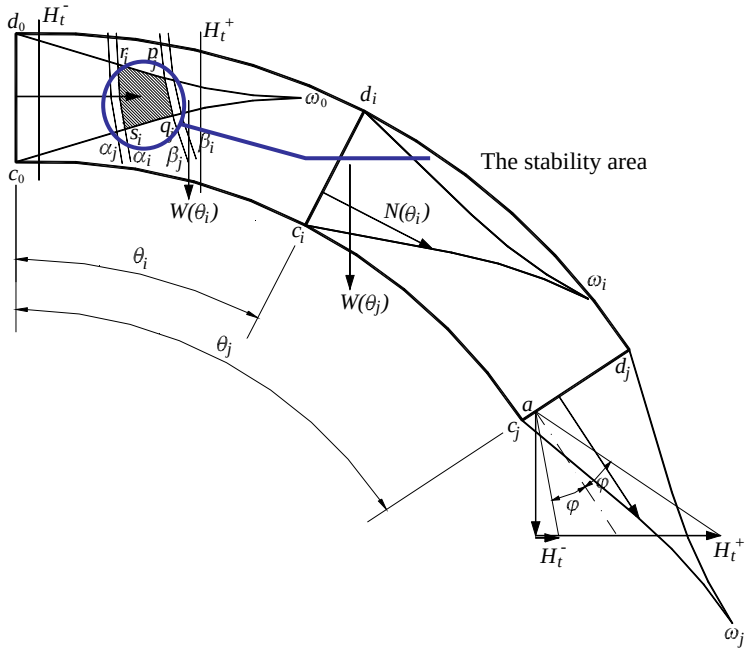

Figure 2. The stability area.

By scanning every joint *i* of the arch and every eccentricity *e*, the set of all admissible thrust values may be found. The locus of the extremes of the vectors representing such forces constitutes the so-called area of stability, *A*, common to all the areas A_i. In Figure 2, for example, it is represented by the curvilinear quadrilateral $r_i s_i p_j q_j$, corresponding to joints $c_i d_i$ and $c_j d_j$. Limiting our investigation to equilibrium and strength, when this area shrinks to a point, the limit condition is attained and a unique admissible thrust line exists.

3.2 *Non-linear elastic analysis*

The alternative method makes use of a simple one-dimensional non-linear elastic model, which relies on the piecewise-linear constitutive relation between longitudinal strains and stresses plotted in Figure 3, where σ_t and σ_c are the material's tensile and compressive strengths, respectively.

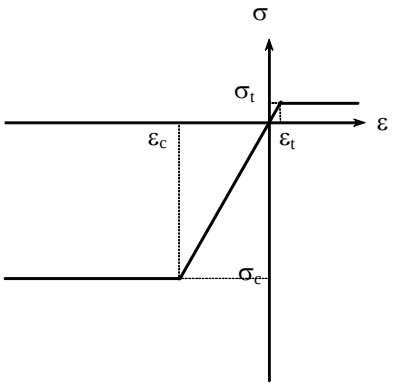

Figure 3. The non-linear stress-strain relation.

Under the assumption commonly accepted in the theory of the bending of beams, namely that any given cross-section remains plane and orthogonal to the line of axis after bending, a non-linear constitutive relation able to roughly describe the complex mechanical behavior of masonry may be established between the axial strain ε_0 and cross-sectional curvature χ, on the one hand, and the axial force N and bending moment M, on the other.

Due to the assumed bounded tensile and compressive strengths, the set of all internal force values compatible with the assumed constitutive relation is a closed bounded domain in the (N, M) plane (Figure 4).

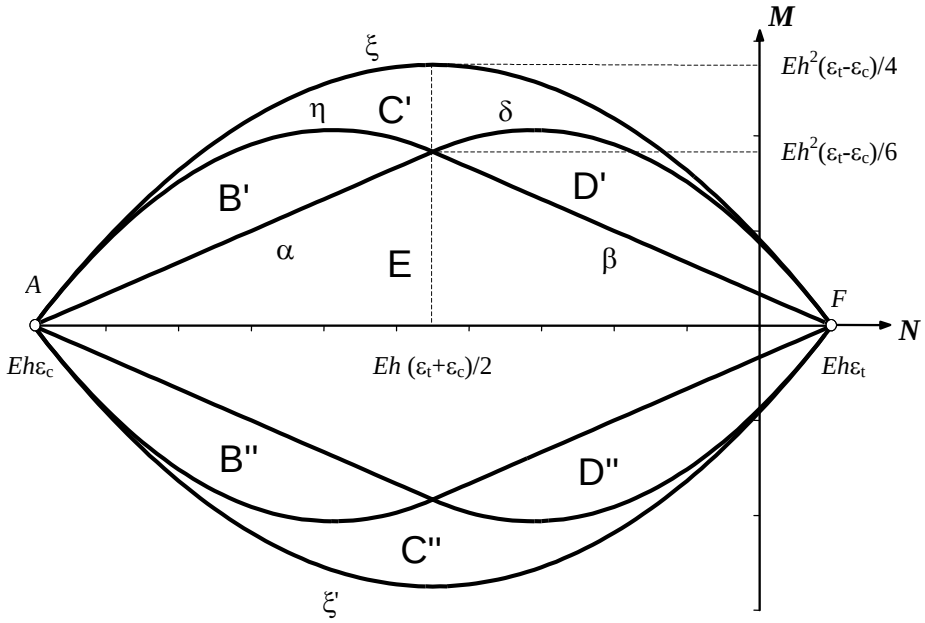

Figure 4. The elastic domain.

Different analytic expressions for the constitutive relation hold in the different regions into which the domain is subdivided. By way of example, in region C' (where the stress distribution is non-linear under both tension and compression), it is

$$\begin{cases} N = \dfrac{E}{8\chi}[(\varepsilon_c - \varepsilon_t)(\varepsilon_t + \varepsilon_c - 2\varepsilon_0) + h\chi(\varepsilon_c + \varepsilon_t)], \\ M = \dfrac{E(\varepsilon_c - \varepsilon_t)}{24\chi^2}[(\varepsilon_c - \varepsilon_t)^2 + 3(\varepsilon_t + \varepsilon_c - 2\varepsilon_0)^2 - 3h^2\chi^2]. \end{cases} \tag{1}$$

Analogous relations, omitted here for the sake of brevity, hold in the other regions.

Simple calculations show that under the foregoing hypotheses, and in the case of a circular arch with radius R, the tangential displacement component u may be expressed as

$$u(\theta) = A + B\sin(\theta) + C\cos(\theta) + \int_{\theta_0}^{\theta}[1 - \cos(t - \theta)][-R^2\chi(t) + R\varepsilon_0''(t)]dt\,, \tag{2}$$

where θ is the angle formed between the radial direction and the horizontal at any point along the line of the arch axis, A, B and C are three constants, and the primes denote differentiation with

respect to θ. Moreover, analogous expressions hold for the radial displacement component *v*, as well as the rotation φ of the cross-section.

Under general load and constraint conditions, equation (2) together with the analogous ones for v and φ lead to a non-linear set of equations in the three constants A, B and C and the redundant end-reaction components. Due to the strong non-linearity of the problem, the solution to this set of equations can be obtained in closed form only for cases of relatively simple loads and geometries. In general, the solution is sought via an iterative method. For the present context, an ad hoc numerical procedure has been used, following a modified standard Newton-Raphson scheme. The arch's behavior is assumed to be linear during any given iteration. In this way, we obtain a linear set of equations, which is solved by performing the required integration numerically. The curvature and axial strain are updated, and the procedure is then repeated until the difference between the values of the internal forces N and M furnished by the constitutive relations and the corresponding ones calculated from the equilibrium equations becomes lower than a small fixed threshold value (for a more detailed illustration of the model see [8]).

4 SOME RESULTS FOR CIRCULAR, POINTED AND ELLIPTICAL ARCHES

The methods described in the foregoing will now be applied to an analysis of the behavior of circular, elliptical and pointed masonry arches. Here, we shall limit ourselves to a brief illustration of some meaningful results.

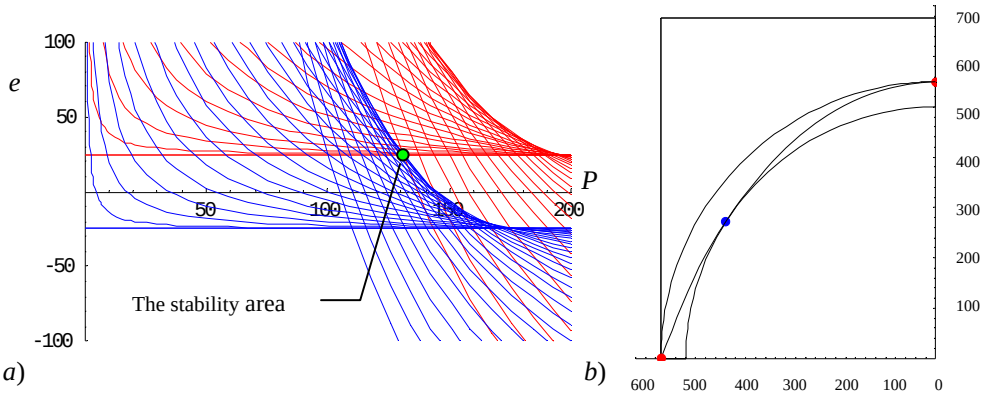

Figure 5. Stability area and line of thrust for a semicircular arch (β = 0° and *h* = 50 cm).

Let us begin with the case of a circular arch with *h* = 50 cm, loaded by a wall with β = 0°. The limit height of the wall compatible with the bearing capacity of the arch is reached when the area of stability (Figure 5a) shrinks to a point. The limit line of thrust for this case is shown in Figure 5b. By fixing the angle β and varying the cross-sectional thickness *h*, we find different values for the maximum height of the wall corresponding to a limit condition, as reported in Figure 6, where the wall height *H* is measured starting from the springings. It is interesting to observe that in some cases, for small values of *H*, we find both a minimum and a maximum height corresponding to a limit equilibrium condition

It is noteworthy that, for any almost *h*, *pointed arches allow for much greater wall heights than circular ones*. From an architectural point of view, such a result is clearly consistent with the greater slenderness of Gothic buildings. It is also rather interesting to note that, for some values of *h*, elliptical depressed arches also afford higher load capacities than circular arches of the same thickness.

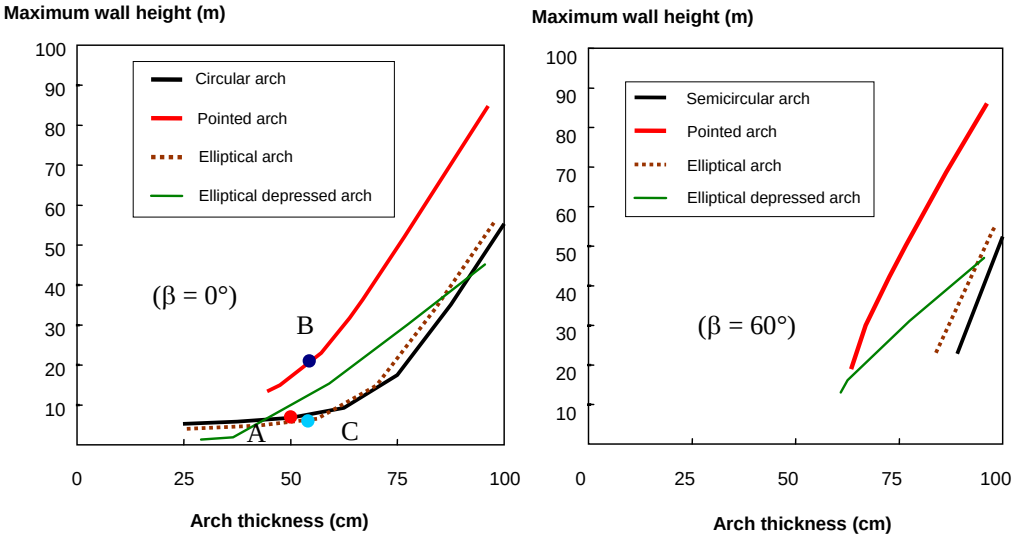

Figure 6. Limit height of the arch-wall system for circular, elliptical and pointed arches (left: β = 0°; right: β = 60°).

The limit height values of the wall obtained by applying the non-linear elastic model to the same loading cases illustrated above are in very good agreement with the corresponding values obtained via the stability area method. In addition, the non-linear elastic analysis enables following the evolution of the displacement and stress fields within the arch, as well as the extension of the non-linear regions as the load increases.

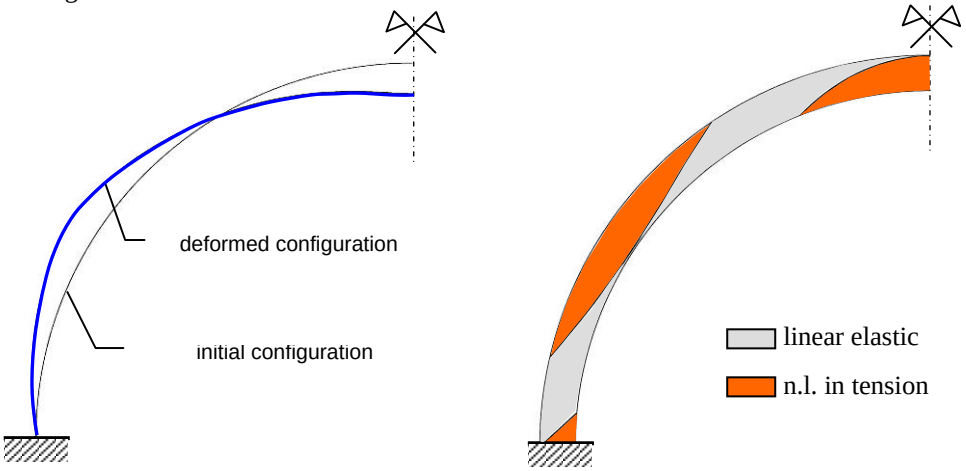

Figure 7. Circular arch: (left) deformed configuration (displacement magnified two times); (right) non-linear regions under tension (in orange).

By way of example, Figure 7 illustrates the deformed configuration and the distribution of non-linear regions at collapse for the circular arch already examined via the stability area method

(point A in Figure 6). The arch has radius R = 5.25 m, cross-sectional height h = 50 cm and it is loaded by its self-weight and the weight of a 6.75m-high wall. By reason of symmetry, only the left half of the arch is shown in the figures.

The height of the wall (the highest value for which convergence of the numerical procedure is achieved) is slightly less than the maximum height as assessed by the stability area method (6.77 m). As is evident from the graph (the crown vertical displacement turns out to be about 21 cm), the displacements in the neighborhood of collapse are not at all negligible. Moreover, wide zones along the arch are in a non-linear regime, thus leading to the supposition that widespread cracking would appear along the arch. The large increase in the magnitude of the displacements as the load approaches its limit value is also confirmed by the plot shown in Figure 8.

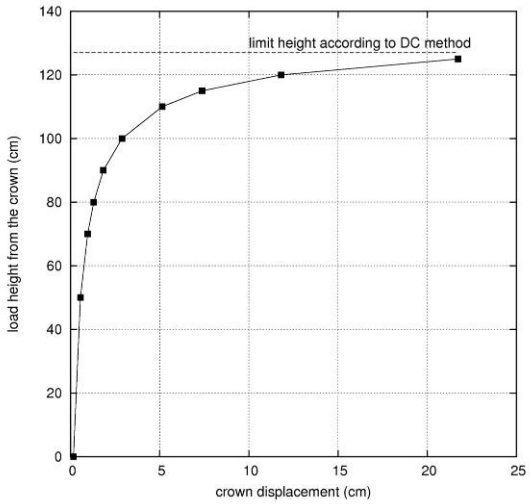

Figure 8. Plot of the crown vertical displacement for different values of the wall height.

A second case of a pointed arch (point B in Figure 6) is illustrated below as an example. The arch has radius R = 10.57 m, and cross-sectional height h = 57.2 cm. The numerical procedure converged at a wall height of 22.85 m (the stability area method yields a limit height of 23 m). Figure 9 shows the diagram of the extrados and intrados stresses, together with the distribution of the non-linear regions at collapse. It should be observed that, in this case, the limit stress under compression is reached in some parts of the arch, and that the distribution of the non-linear regions is now quite different from that found in the previous case of a circular arch, thus leading to the suspicion that in this case local crushing phenomena are likely to appear.

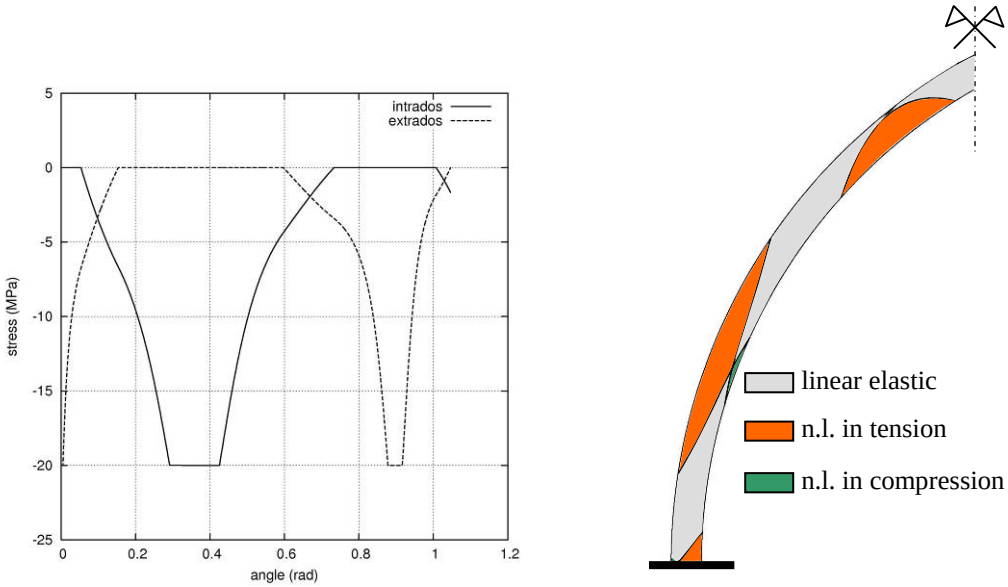

Figure 9. Pointed arch: (left) extrados and intrados stresses;
(right) extension of the non-linear regions along the left half of the arch.

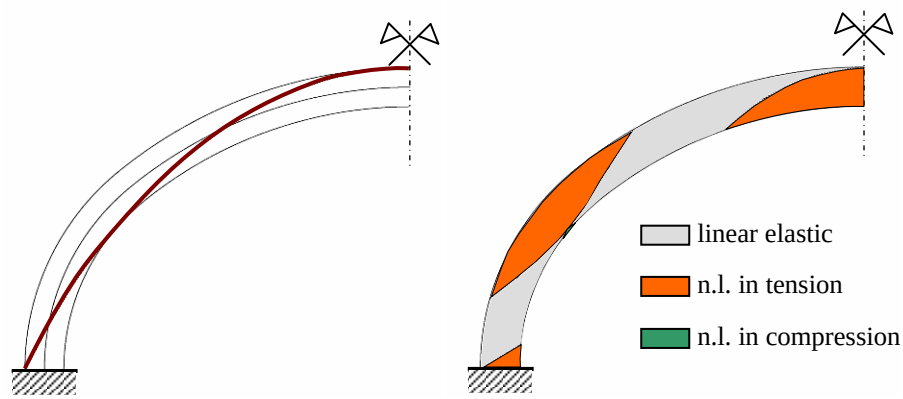

Figure 10. Elliptical arch: (left) line of thrust;
(right) extension of the non-linear regions along the left half of the arch.

Lastly, the case of an elliptical arch (point C in Figure 6) is illustrated below. The arch has cross-sectional height h = 56.2 cm; the line of axis is approximated by two arches of circles with radius R = 3.38 m and R = 6.39 m, respectively. The numerical procedure converged at a wall height of 6.06 m (the stability area method yields a limit height of 6.57 m). Figure 10 shows the line of thrust and the distribution of the non-linear regions at collapse. It should be observed that, once again in this case, the displacements in the neighborhood of collapse are considerable (the crown vertical displacement turns out to be about 35 cm). Moreover, wide zones along the arch are in a non-linear regime in tension and a small portion of the intrados of the arch is in a non-linear regime in compression, thus leading to the supposition that widespread cracking, as well as some local crushing phenomena are also probable in this case.

5 CONCLUSIONS

The load-bearing capacities and the mechanical response of circular, elliptical and pointed arches loaded by their self-weight and by the weight of an overlying wall have been evaluated by means of the stability area method and non-linear elastic analysis. As already observed in previous cases studied by the authors [5], the results obtained via these two methods of analysis turn out to be in excellent agreement, except for very few special cases. Moreover, the two methods perform complementary functions: the stability area method allows for readily determining the collapse load value, while the non-linear elastic analysis provides a helpful and, in some aspects, essential check of its mechanical significance by following the evolution of the displacement field and extension of the non-linear regions, where cracking and crushing phenomena arise as the load increases.

Some concluding remarks now seem in order. The wide extension of the non-linear regions, as well as the large magnitude of the displacements when the arches are close to collapse suggest that neglecting the effects of both the material and geometrical non-linearities could lead to dangerous overestimation of the actual value of the collapse load. In other words, it appears that the non-linear elastic model utilized needs to be modified in order to also expressly account for the geometrical non-linearities consequent to the emergence of the all-but-negligible displacements as the system approaches collapse. Moreover, as shown in another work [6], lacking a sufficiently accurate evaluation of the real distribution of the loads transmitted to the arch by the overlying wall, we cannot hope to make a reliable determination of the collapse load for an arch-wall system. Finally, it seems advisable to supplement the system collapse load value determined via any standard application of limit analysis with a conventional reduced value, so as to introduce a condition that makes reference, for example, to the attainment of a limit residual stiffness value, below which the arch's equilibrium is to be regarded as very uncertain.

References

[1] Alfano G., Rosati L., Valoroso N., "A numerical strategy for finite element analysis of no-tension materials", *Int. J. Numer. Meth. Engng*; **48**, 317-350 (2000).

[2] Lourenço P.B., "Assessment, diagnosis and strengthening of Outeiro Church, Portugal", *Construction and Building Materials*, **19**, 634–645 (2005).

[3] Aita D., Foce F., "The masonry arch between limit and elastic analysis. A critical re-examination of Durand-Claye's method", *Proc. First Int. Congress on Construction History*, S. Huerta (ed.), Instituto Juan de Herrera, Madrid 2003, vol. II, 895-905 (2003).

[4] Bennati S., Barsotti R., "Optimum radii of circular masonry arches", *Third International Arch Bridges Conference – ARCH 01*, vol. 1, 489-498, Paris, France (2001).

[5] Aita D., Barsotti R., Bennati S., Foce F., "Collapse of masonry arches in Romanesque and Gothic constructions", *Proc. Arch Bridges ARCH'07*, Madeira (2007).

[6] Barsotti R., Bennati S., Dami A., "A simple structural model for a masonry arch-wall system subjected to dead vertical loads", *Proc. AIMETA09*, Ancona (2009).

[7] Aita D., Barsotti R., Bennati S., Foce F., "The statics of pointed masonry arches between 'limit' and 'elastic' analysis", *Proc. Arch Bridges ARCH'04*, 353-362, P. Roca and E. Oñate (Eds), Barcelona, CIMNE, (2004).

[8] Barsotti R., Bennati S., "Non-linear analysis and collapse of masonry arches: a simple and effective one-dimensional model", forthcoming paper.